



# *In silico* validation of coumarin derivatives as potential inhibitors against Main Protease, NSP10/NSP16-Methyltransferase, Phosphatase and Endoribonuclease of SARS CoV-2

Akhilesh Kumar Maurya and Nidhi Mishra

Chemistry Laboratory, Department of Applied Sciences, Indian Institute of Information Technology Allahabad, Devghat, Jhalwa, Prayagraj, UP, India

Communicated by Ramaswamy H. Sarma

## ABSTRACT

Coronavirus Disease (COVID-19) is recently declared pandemic (WHO) caused by Severe Acute Respiratory Syndrome Coronavirus 2 (SARS-CoV-2). The virus was named Severe Acute Respiratory Syndrome Coronavirus 2 (SARS-CoV-2), (Coronavirus Disease 2019). Currently, there is no specific drug for the therapy of COVID-19. So, there is a need to develop or find out the new drug from the existing to cure the COVID-19. Identification of a potent inhibitor of Methyltransferase, Endoribonuclease, Phosphatase and Main Protease enzymes of SARS CoV-2 by coumarin derivatives using *insilico* approach. The *in silico* studies were performed on maestro 12.0 software (Schrodinger LLC 2019, USA). Two thousand seven hundred fifty-five biologically active coumarin derivative was docked with above receptor proteins of SARS CoV-2. The molecular dynamic simulation of the top one ligand of respected proteins was performed. Top five ligands of each protein were taken for study. Coumarin derivatives actively interact with taken receptors and showed good docking results for Methyltransferase, Endoribonuclease, Phosphatase and Main Protease and top five compounds of each have docking score from  $-9.00$  to  $-7.97$ ,  $-8.42$  to  $-6.80$ ,  $-8.63$  to  $-7.48$  and  $-7.30$  to  $-6.01$  kcal/mol, respectively. The docked compounds were showed RMSD and binding stability of simulated ligands are show the potency of ligands against the SARS CoV-2. Our study provides information on drugs that may be a potent inhibitor of COVID-19 infection. Drug repurposing of the available drugs would be great help in the treatment of COVID-19 infection. The combination therapy of the finding may improve inhibitory activity.

## HIGHLIGHTS

- Coronavirus Disease (COVID-19) is recently declared pandemic (WHO) caused by Severe Acute Respiratory Syndrome Coronavirus 2 (SARS-CoV-2).
- *In silico* virtual screening, docking, ADME, MM-GBSA and MD simulation analysis of coumarin derivatives against Methyltransferase (MTase), Endoribonuclease(endoU), ADP ribose Phosphatase and Main Protease enzyme of SARS CoV-2.
- All the analysis was performed on Maestro 12.0 Schrodinger software against respective receptors.
- Top five compounds of coumarin derivatives s docked at the active site of Methyltransferase (MTase), Endoribonuclease(endoU), ADP ribose Phosphatase and protease and top five compounds of each have docking score from  $-9.00$  to  $-7.97$ ,  $-8.42$  to  $-6.80$ ,  $-8.63$  to  $-7.48$  and  $-7.30$  to  $-6.01$  kcal/mol, respectively, of SARS CoV-2.
- These compounds were used to analysis of binding free energy by using the Prime MM-GBSA module.
- All the compounds showed drug-likeness properties.
- MD simulation of Proteins and ligands showed binding stability and good RMSD, radius of gyration of protein, coulomb-SR and LJ-SR energy.

## ARTICLE HISTORY

Received 16 June 2020  
Accepted 30 July 2020



## KEYWORDS


SARS CoV-2; docking; ADME/T; binding free energy; MD simulation; inhibitor

## 1. Introduction

Coronaviruses are medically and veterinary important viruses. They have lipoprotein envelopes with single-stranded RNA and enter in host cells with help of class I fusion protein (Masters, 2006). They include human coronaviruses (SARS-CoV) severe acute respiratory syndrome coronavirus, porcine

epidemic diarrhea virus (PEDV), transmissible virus (TGEV), MERS-CoV (Middle East respiratory syndrome coronavirus) (Masters, 2006). Recently in December-2019, many patients were suffering from unknown pneumonia and dry cough in Wuhan city, Hubei province, China (Huang et al., 2020), a new coronavirus, named as novel coronavirus-2019 (nCoV-2019) on 7 January 2020, by the World Health Organization

**CONTACT** Nidhi Mishra  [nidhimishra@iiita.ac.in](mailto:nidhimishra@iiita.ac.in)  Chemistry Laboratory, Department of Applied Sciences, Indian Institute of Information Technology Allahabad, Prayagraj, UP 211012, India

 Supplemental data for this article can be accessed online at <https://doi.org/10.1080/07391102.2020.1808075>

© 2020 Informa UK Limited, trading as Taylor & Francis Group

(WHO) (Huang et al., 2020). Later, the virus was renamed Severe Acute Respiratory Syndrome Coronavirus 2 (SARS-CoV-2), COVID-19 (Coronavirus Disease 2019) caused by the SARS-CoV-2. The zoonotic origin of SARS-CoV-2 has been implicated by phylogenetic data analysis (Lu et al., 2020). On 11 March 2020, the COVID-2019 disease outbreak declared pandemic (WHO, 2020a). According to the latest data, confirmed cases of COVID-2019 disease are 69,31,000 confirmed deaths 4,00,557 in 216 countries worldwide (WHO, 2020b) and the number of confirmed cases on India reached 2,6700 of which 7466 were dead and 1,29,214 cured (Ministry of Health and Family Welfare India, 2020). Currently, we do not have any specific drugs for the treatment of COVID-2019 patients. Some potential combinations of protease inhibitors like lopinavir/ritonavir commonly used in the treatment of HIV and other antiviral inhibitors like remdesivir, tenofovir disoproxil are using for the treatment of COVID-2019 patient (Wang et al., 2020).

Methyltransferase of SARS CoV-2 involves mRNA capping and cap by 2'-O-ribose methylation to the 5'-cap structure of viral mRNAs. NSP10/NSP16 is a binding site of the N7-methyl guanosine cap. So, NSP10/NSP16 Methyltransferase plays an important role in viral mRNAs cap methylation (Swiss-Model, <https://swissmodel.expasy.org/repository/species/2697049>).

Endoribonuclease enzyme of all known CoVs is highly conserved (Deng & Baker, 2018; Deng et al., 2019). Endoribonuclease enzyme of coronaviruses is similar to the animal cellular Endoribonuclease. It plays a role in mRNA maintenances (Joseph et al., 2007; Snijder et al., 2003). Adenosine diphosphate ribose Phosphatase (ADRP) domain of SARS CoV nsP3 is indeed a Phosphatase that removes the terminal 1'' phosphate from ADP-ribose-1''-phosphate (Appr-1''-p) from the tRNA so it plays an essential role in the translation of SARs CoV (Saikatendu et al., 2005). CoV S (coronavirus spike glycoprotein) proteins are class I viral fusion proteins, and for the fusion with human body cells activation of S protein is required and protease cleavage is required for S protein activation (Ou et al., 2016). So, all taken enzymes or receptors very actively participate in the replication and infection of SARS CoV-2, and inhibition of these targets may inhibit the infection of SARS CoV-2 or may cure the infected people with COVID-19.

Therefore, it is assume that targeting Main Protease, NSP10/NSP16 Methyltransferase, Phosphatase and Endoribonuclease of SARS CoV-2 by a potential inhibitor molecule may offer big assurance to break the growth and infection of the coronavirus within the host body. However, potential drug discovery and experimental testing are very demanding to forward this emergency. On this subject, repurposing of molecules/drugs might be quite helpful as it would introduce lead molecules from the pool of previously exiting medicine. This finally saves the cost and time prescribed for the animal and human trials for the firing of any novel drugs and various unavoidable legal practices before to commercialization and use in human applications (Elmezayen et al., 2020; Pawar, 2020; Senanavake, 2020; Shah et al., 2020). Thus, *in silico* virtual screening of potential drugs of Main Protease, NSP10/NSP16 Methyltransferase,

Phosphatase and Endoribonuclease of SARS CoV-2 was performed by considering more than 2755 bioactive molecules of coumarin derivatives. Admittance of the bioactive compounds offers the scope of finding effective drugs with minimum side effects.

The scientist has designed various antiviral drugs by synthetic methods and nature have thousands of drugs in the form of medicinal plant, fungi, algae and other natural resources. The various plant contains coumarin and its derivatives known as natural coumarins like Rutamarin, Frutinone A, Floroselin obtained from *Rutagraveolens*, *Polygala fruticose*, *Seselisessiliflorum*, respectively (Murray, 2002), etc. Chemically synthesised coumarins are coumarin, 8-nitro-7-hydroxycoumarin (Egan et al., 1997), 4-formylcoumarin (Nicolaidis et al., 1996), 8-hydroxy-7-phenylaminocoumarin (Bezergiannidou-Balouctsi et al., 1993), etc.

Coumarin derivatives have been used as an antiviral agent in various viral disease such as 2-[(6-bromocoumarin-3-yl) methylenethio]-5-fluorobenzimidazole and its derivative 1-[(2, 3, 4, 6-tetra-O-acetyl) glucopyranos-1-yl] – 2-[(6-bromocoumarin-3-yl) methylenethio] benzimidazole as anti-hepatitis C (Bezergiannidou-Balouctsi et al., 1993), N-benzylated coumarin-AZT conjugates inhibits HIV protease and reverse transcriptase (Hwu et al., 2008), bis-(triazolothiadiazinyl coumarin) as anti-influenza agent (Olomola et al., 2013; Pavurala et al., 2018), etc. In the present study, we have done the *in silico* screening of coumarin derivatives against protease, NSP15 endonuclease, ADP ribose of Phosphatase NSP3 and Methyltransferase NSP10/NSP16 of SARS-CoV-2. The outputs of the present study will provide information to other researchers with opportunities to identify the accurate drug for treating COVID-19.

## 2. Experimental

### 2.1. Material and methods

The *in silico* studies were performed on Lenovo ThinkPad which has 12 GB RAM, 1TB hard disk, Intel i7 generation with 6 cores. Molecular docking was performed on GLIDE (Grid-based Ligand Docking with Energetics) module of maestro 12.0 (Schrodinger LLC 2019, USA) between ligand/s molecules with a receptor macromolecule, mainly protein.

### 2.2. Ligand preparation

Some coumarin derivatives, both naturally derived and chemically derived were found to have good antiviral activity. Based on biological activity 2755 compounds of coumarin derivatives and experimentally proved drugs Remdisiver and Hydroxychloroquine for COVID-19 were downloaded from the website PubChem (<https://pubchem.ncbi.nlm.nih.gov/#query=coumarin>), a chemical database in SDF format. These ligands were prepared using the LigPrep, Glide-v8.3 Schrodinger, LLC, New York, NY, 2019-2 (Ligprep & Macromodel, 2011). LigPrep performs 3D low energy structure conversion from 2D with accurate chiralities. Ionization was retained in original states with realistic bond lengths

and bond angles, tautomers, ring conformation were generated, using the OPLS-2005 force field.

### 2.3. Protein preparation

The protein structures, namely, PDB ID: 6W61 (NSP16/NSP10 Methyltransferase complex o), PDB ID: 6VWW (NSP15 Endoribonuclease), PDB ID: 6VXS (ADP ribose Phosphatase [ADRP] of NSP3) and PDB ID 6LU7 (Main Protease) were retrieved from protein data bank (<https://www.rcsb.org/>) as anti-COVID-2019 targets. Retrieved structures were subjected to the protein preparation wizard of Maestro for preparation of the structures (Glide v8.3, Schrodinger, LLC, New York, NY, 2019-2). The selected structures were processed for the incorporation of creating zero bond order for metal, assigning proper bond orders, creating disulphide bonds and the addition of missing hydrogens. Optimization of hydrogen bonds was assigned using sample water orientations and Non-hydrogen atoms of protein structures were energetically minimized until the RMSD (root mean square deviation) reaches the value of 0.3 Å.

### 2.4. Generation of receptor grid

Cocrystallized structures of the target proteins were downloaded from the PDB databank. The partial atomic charge cutoff was 0.25 and van der Waals radii of receptor atoms were 1.0 Å by defaults. The centroid of the workspace ligand has an enclosing box to represent the activity of the receptor/s. Center of the bound ligand in receptor/s was selected to generate a grid box by using the above protocol in the receptor grid generation module of Maestro Glide v8.3, Schrodinger, LLC, New York, NY, 2019-2.

### 2.5. Virtual screening and molecular docking

Virtual screening of prepared coumarin derivatives was performed using virtual screening workflow (VSW) of GLIDE (Glide v8.3, Schrodinger, LLC, New York, NY, 2019-2) (Wizard et al., 2009). Running QuikProp, prefilters by Lipinski rule and remove ligands with reactive function groups were selected in VWS for filtering the ligands. VWS of Glide has three levels of Choose a docking precision, HTVS (High Throughput Virtual Screening), standard-precision (SP), Extra-precision (XP). Extra precision (XP) docking was performed on coumarin derivatives by keeping parameters of the scaling factor at 0.80 and partial charge cutoff at 0.15. Five percent best docked result was kept for further study. The binding affinity of docked compounds for the receptors, of NSP16/NSP10 Methyltransferase complex, NSP15 Endoribonuclease, ADP ribose Phosphatase of NSP3 and Main Protease, the active site was calculated from the docking binding energy.

$$\begin{aligned} \text{GScore} = & 0.065 \times \text{van der Waals energy} + 0.130 \\ & \times \text{Coulomb energy} + \text{Lipo} + \text{H bond} \\ & + \text{Metal} + \text{BuryP} + \text{RotB} + \text{Site} \end{aligned}$$

where,

Lipo = hydrophobic interactions, Metal = metal binding, BuryP = buried polar group penalty, RotB = penalty for freezing rotatable bonds and Site = polar interactions existing in the active site represented.

### 2.6. Binding free energy calculation

Binding free energy of docked ligands was predicted using the Prime Molecular Mechanics-Generalized Born Surface Area (MM-GBSA) approach of Glide v8.3, Schrodinger, LLC, New York, NY, 2019-2, which includes the OPLS\_2005 molecular mechanics energies, nonpolar term of solvation and VSGB solvent model (Li et al., 2011; Maurya et al., 2020). Pose viewer file (generated after docking) was used to performed Prime MM-GBSA of lead molecules to calculate binding free energy. The following descriptors were used to calculate changes in energy upon binding.

DG bind = Ligand binding free energy,  $E_{\text{complex}}$  = complex free energy,  $E_{\text{protein}}$  = free energy of the receptor without the ligand,  $E_{\text{Ligand}}$  = unbound ligand-free energy.

$$\text{DG bind} = E_{\text{complex}} - E_{\text{ligand}} - E_{\text{receptor}}$$

### 2.7. ADME/T studies

Absorption, distribution, metabolism, excretion and toxicity (ADME/T) properties studies reveal the medicinal properties of drugs. QikProp-V6.0 tool in VSW (maestro 12.0) calculated the ADME/T (auxiliary, physicochemical, biochemical, pharmacokinetics and harmfulness properties) information of ligands.

### 2.8. Molecular dynamic simulation

Docked complex of protein and ligand; Main Protease (PDB ID: 6LU7-Pubchem ID: 101223868), nsp10/nsp16 Methyltransferase (PDB ID: 6W61-Pubchem ID: 101223868), NSP15 Endoribonuclease (PDB ID: 6VWW -Pubchem ID: 44406281), ribose Phosphatase (PDB ID: 6VXS -Pubchem ID: 54730083) were selected to perform the molecular dynamic (MD) simulation. GROMACS-18 (Berendsen et al., 1995) software was used to perform MD Run on the central computation facility of the Indian Institute of Information Technology Allahabad on the Linux operating system. The Charmm36 force field was used to simulate the complex structures that employed the sustainability of ligand in the binding pocket of the respective proteins. TIP3P model water molecule was selected in the generation of protein topology files of the charmm36 force field (Mark & Nilsson, 2001). The ligand topology file was generated by using the CGenFF server and Charmm36\_mar2019 force field (Vanommeslaeghe & MacKerell, 2012). The complex of protein and ligand was constructed using the GROMACS tutorial. A dodecahedron nm box edge was generated to solvate the system. The aqueous environment was created using the SPC water model (Berendsen et al., 1981). Na<sup>+</sup> and Cl<sup>-</sup> ions were used to neutralize the system according to charge in the solvent. The energy minimization of each system was minimized with 5000 interaction by using the steepest descent algorithm

**Table 1.** Docking score, Gibbs binding free energy score of docked ligand–protein complex.

S. N.	PubChem CID	Interacted amino acid	Docking score kcal/mol	Glide emodel kcal/mol	Glide energy kcal/mol	Gibbs binding free energy kcal/mol
<b>NSP10/NSP16 Methyltransferase</b>						
1	101223868	A: met248, A; thr48,	−9.00	−66.68	−50.41	−69.61
2	688485	B:thr48, glu61	−8.51	−67.36	−51.74	−58.58
3	53393956	A: gln88, pro252	−8.27	−87.18	−59.73	−76.74
4	10781960	A: met248, gln88, B; thr48	−8.09	−62.59	−45.36	−58.89
5	102214788	A: gln88, B; glu61	−7.97	−60.22	−39.98	−60.33
Standard	Remdisivir	A: asp69, asp97, tyr69, leu98	−6.52	−	−	−
	Hydroxychloroquine	A: lys69, asp69, asp97,	−6.71	−	−	−
<b>Endoribonuclease</b>						
1	44406281	A: glu69, lys71, asn200, thr275, tyr279, asp297	−8.42	−54.43	−40.50	−56.22
2	25128696	A: lys71, leu201, ser274, thr275,asp297	−7.69	−58.90	−46.17	−61.82
3	101223868	A: lys71, ser274, thr275, asp297	−7.32	−55.19	−42.09	−58.96
4	22203	A: lys90, asp268, asp 297	−6.92	−52.76	−41.33	−59.04
5	5362190	A: lys71, asp273, ser274, asp297	−6.80	−53.76	−37.63	−54.00
Standard	Remdisivir	A: tyr89, lys90, gly165, thr169, ser198, arg199, leu201	−7.66	−	−	−
	Hydroxychloroquine	A: asp 268, thr275, tyr279, asp 297	−5.24	−	−	−
<b>Phosphatase</b>						
1	54730083	B: ala38, ala50, leu126	−8.63	−61.51	−45.62	−59.05
2	53393956	B: lys44, val49, thr71, leu126, ala 129	−8.22	−64.09	−49.41	−76.32
3	3758198	B: leu126, phe156	−7.81	−58.89	−44.49	−72.24
4	88279989	B: ala50, leu126	−7.72	−56.87	−35.43	−64.25
5	5359550	B: leu126, ala154, asp157	−7.48	−44.97	−39.33	−72.09
Standard	Remdisivir	B: asp135, phe156, asp157,	−2.38	−	−	−
	Hydroxychloroquine	B: ile23, ala129	−4.86	−	−	−
<b>Main Protease</b>						
1	101223868	A: gln110, ile 246	−7.30	−45.27	−35.70	−58.67
2	9818076	A: gln107, pro108, glu140	−6.33	−47.59	−35.43	−59.83
3	43000	A: pro108, glu240, hie246	−6.24	−36.81	−29.68	−43.27
4	11616886	A: glu240, hie246	−6.23	−43.30	−34.01	−65.34
Standard	Remdisivir	A: ile 246	−3.23	−	−	−
	Hydroxychloroquine	A: Ser46	−1.75	−	−	−

1000 kJ mol<sup>−1</sup> nm<sup>−1</sup>. After the energy minimization, the ligand was restrained with their position and the system was subjected to equilibration with 1 bar pressure and 310 K temperature at 2 femtosecond (fs) stem time (Hess et al., 2008).

The non-bonded pair list and the LINCS constrains algorithms were used to position restraint conditions for the heavy atoms (Jorgensen & Duffy, 2002). Particle mesh Ewald method was used to calculate electrostatic interactions. Berendsen temperature coupling method was used to regulate the temperature inside the system (Berendsen et al., 1981). Finally, the systems were subjected to MD Run for duration of 60 nanoseconds (ns). After the completion of MD simulation, trajectories were analyzed and observe the structural deviation ligand and protein. The root mean square deviation (RMSD), Radius of gyration (Rg), Coulumb-SR energy and LJ-SR energy were calculated.

### 3. Result and discussion

In the present study, NSP10/NSP16 Methyltransferase, Endoribonuclease, ADP ribose Phosphatase and Main Protease were evaluated through molecular docking studies with coumarin derivatives, which is an *in silico* analysis, using Glide module of Schrodinger.

#### 3.1. Virtual screening and molecular docking of coumarin derivatives

Coumarin derivatives (2755 compound) were docked at the active site of NSP10/NSP16 Methyltransferase (MTase), Endoribonuclease

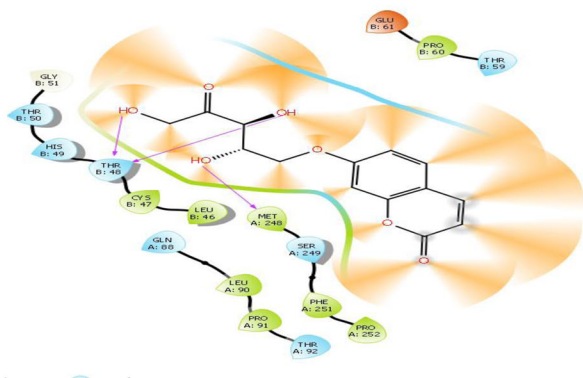
(endoU), ADP ribose Phosphatase and Main Protease and top five compounds with the best conformation of each have docking score from −9.00 to −7.97, −8.42 to −6.80, −8.63 to −7.48 and −7.30 to −6.01 kcal/mol, respectively (Table 1). Closer view of the interaction of ligands and each SAR CoV-2 proteins/receptors discloses that the oxygen and nitrogen-containing compounds of coumarin derivatives are interacting with active site's amino acids of receptors, H atom of hydroxy groups make coumarin derivatives more suitable to form a hydrogen bond with the target macromolecule and hydrophobic interaction with amino acids of binding site show the good docking score. Glu, Gln and Thr amino acid residues are mainly form hydrogen bonding with chain A of NSP10/NSP16 Methyltransferase. The docking score of ligands PubChem ID: 101223868, 688485, 53393956, 10781960 and 102214788 with Methyltransferase are −9.00, −8.51, −8.27, −8.09 and −7.97 kcal/mol, respectively (Figure 1 and Table 1), while experimentally proved standard drugs Remdisivire and Hydroxychloroquine was showed less docking score −6.52 and −6.71 kcal/mol than the best five docked coumarin derivatives. 3D representation of pocket of active site of Methyltransferase receptor with ligands (mesh surface and solid surface) given in Supporting Information (see Figure S1). Chain A binding pocket aminoacids Glu, Asn, Lys, Thr, Asp and Ser of Endoribonuclease making hydrogen bonds with docked ligands. Ligands with PubChem ID: 44406281, 25128696, 101223868, 22203 and 5362190 showed docking score −8.42, −7.69, −7.32, −6.92 and −6.80 kcal/mol, respectively, and standard drugs Remdisivire and Hydroxychloroquine −7.66 and 5.28 kcal/mol with Endoribonuclease (Figure 2 and Table 1). Three dimensional representation of pocket of active site of Endoribonuclease receptor

Table 2. ADME/T properties of top five compounds of each receptors and ADME/T Score of ligands.

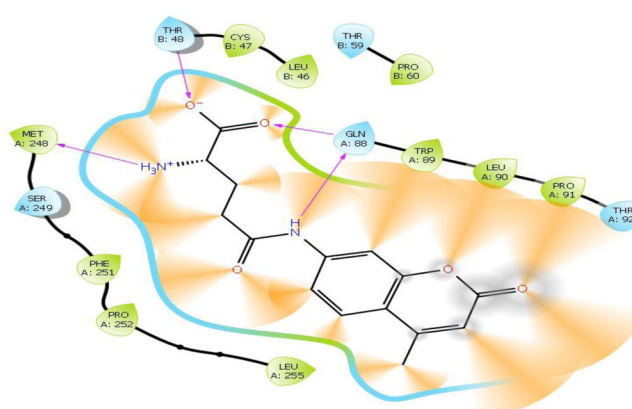
S. N.	PubChem CID	IUPAC name of compounds	MW	Log s	Logo/w	Accept	H	Donor	H	QPP	Caco	QPllog	BB	%Human Oral/Abs	Qplog	HERG	SASA	FOSA	FISA	PISA	QPllogHERG	ADME/T Score
<b>NSP10/NSP16</b>																						
<b>Methyltransferase</b>																						
1	101223868	7-[(2S,3S)-2,3,5-trihydroxy-4-oxopentoxyl]-1-benzopyran-2-one	294.26	-1.66	-0.23	9.35	2	53.38	-2.18	56.48	-4.89	534.89	98.09	239.21	197.58	-4.89	12					
2	688485	(2S)-2-amino-5-[(4-methyl-2-oxo-1-benzopyran-7-yl)amino]-5-oxopentanoic acid	304.30	-2.48	-1.80	8	4	2.00	-1.95	21.78	-3.94	569.23	155.73	263.12	150.37	-3.94	10					
3	53393956	N'-hydroxy-N-(4-methyl-2-oxo-1-benzopyran-7-yl)octanediamide	346.38	-2.97	0.35	9.2	3	22.28	-2.74	53.13	-4.47	688.09	285.76	250.98	151.34	-4.47	11					
4	10781960	6-[(4-phenyl-1-piperazinyl)methyl]-1-benzopyran-2-one	320.39	-3.27	2.90	5.5	0	468.59	0.10	91.76	-6.76	606.13	164.05	76.13	365.94	-6.76	13					
5	102214788	3,4,5-trihydroxybenzoic acid (2-oxo-1-benzopyran-4-yl) ester	314.25	-2.91	0.35	7.25	3	32.92	-2.17	56.18	-5.33	536.74	0	261.34	275.39	-5.33	13					
<b>Endoribonuclease</b>																						
1	44406281	3-(3,5-dihydroxyphenyl)-6,8-dihydroxy-1-benzopyran-2-one	286.24	-2.70	0.31	5.5	4	24.90	-2.23	53.75	-4.98	507.96	0	274.13	233.82	-4.98	12					
2	25128696	4-[(3,4-dihydroxy-2-methoxyphenyl)thio]-1-benzopyran-2-one	316.32	-3.51	2.22	4.75	2	293.75	-1.12	84.15	-4.99	529.96	83.159	161.12	264.55	-4.99	12					
3	101223868	7-[(2S,3S)-2,3,5-trihydroxy-4-oxopentoxyl]-1-benzopyran-2-one	294.26	-1.66	-0.23	9.35	2	53.38	-2.18	56.48	-4.89	534.89	98.096	239.21	197.58	-4.89	12					
4	22203	8-[3-(dimethylamino)propoxyl]-3-pyridin-4-yl-1-benzopyran-2-one	324.37	-2.67	2.46	6.75	0	365.23	-0.29	87.23	-6.86	642.93	249.91	87.55	305.47	-6.86	13					
5	5362190	(6,7-dihydroxy-4-methyl-2-oxo-1-benzopyran-8-yl)methyl-diethylammonium;chloride	277.31	-1.78	1.07	6	2	97.39	-0.73	68.82	-4.90	534.17	303.03	148.082	83.06	-4.90	12					
<b>Phosphatase</b>																						
1	54730083	4-hydroxy-7-(2-hydroxy-3-phenoxypropoxy)chromen-2-one	328.32	-3.87	2.28	6.45	2	282.91	-1.59	84.20	-6.49	615.41	75.13	162.84	377.43	-6.49	13					
2	53393956	N'-hydroxy-N-(4-methyl-2-oxochromen-7-yl)octanediamide	346.38	-2.97	0.35	9.2	3	22.28	-2.74	53.13	-4.47	688.09	285.76	250.98	151.34	-4.47	11					
3	3758198	3-[2-[(4,5-dimethoxy-3-oxo-1H-2-benzofuran-1-yl)amino]-1,3-thiazol-4-yl]chromen-2-one	436.43	-4.85	2.85	9	1	605.02	-0.82	93.45	-5.96	677.49	190.35	128.03	305.87	-5.96	13					
4	88279989	7-[(4-chloro-6-methoxy-1,3,5-triazin-2-yl)amino]-3-phenylchromen-2-one	380.79	-5.26	3.59	6	1	808.94	-0.63	100	-6.18	631.12	84.30	114.73	355.87	-6.18	13					
5	5359550	(6,7-dihydroxy-4-methyl-2-oxochromen-8-yl)methyl-bis(2-hydroxyethyl)azanium;chloride	309.31	-0.84	-0.74	9.4	4	13.11	-1.78	42.57	-4.84	546.82	225.93	239.89	80.99	-4.84	11					
<b>Main Protease</b>																						
1	101223868	7-[(2S,3S)-2,3,5-trihydroxy-4-keto-pentoxyl]coumarin	294.26	-1.66	-0.23	9.35	3	53.382	-2.185	56.48	-4.89	534.89	98.09	239.21	197.58	-4.89	12					
2	9818076	7-[(3-anilinoethylamino)methyl]coumarin	308.37	-3.67	3.10	5	2	327.696	-0.434	90.15	-7.48	640.12	145.25	92.51	402.36	-7.48	13					
3	43000	3-amino-4-anilino-coumarin	252.27	-3.08	1.99	4	2	604.318	-0.742	88.39	-5.30	482.40	0	128.08	354.31	-5.30	12					
4	11616886	7-(3-chlorobenzyl)oxy-4-(methylaminomethyl)coumarin	329.78	-3.99	3.14	4.75	1	352.046	-0.072	90.92	-6.78	614.36	152.66	89.23	300.85	-6.78	13					
5	23618487	7-[3-(dimethylamino)propoxyl]-3-(4-pyridyl)coumarin	324.37	-2.81	2.45	6.75	0	342.044	-0.351	86.67	-7.02	650.63	251.51	90.55	308.56	-7.02	13					



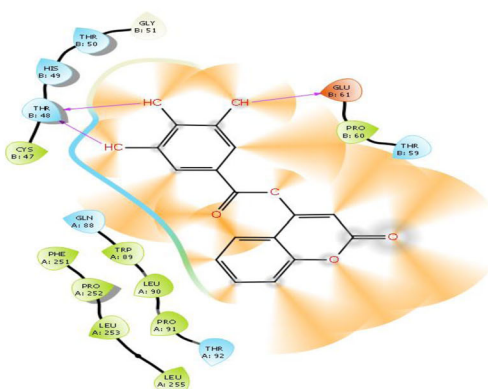
## 101223868 - 6w61 - minimized



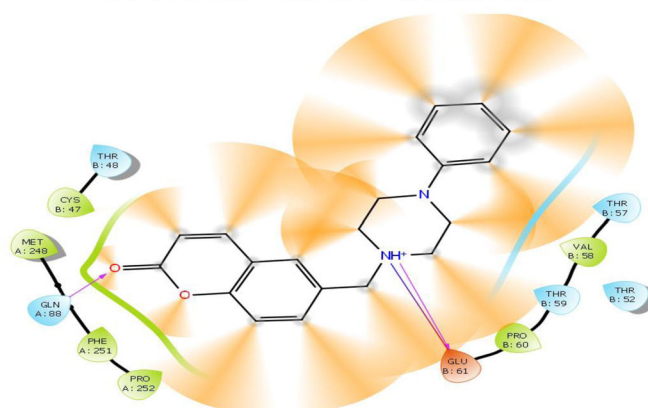
## 688485 - 6w61 - minimized



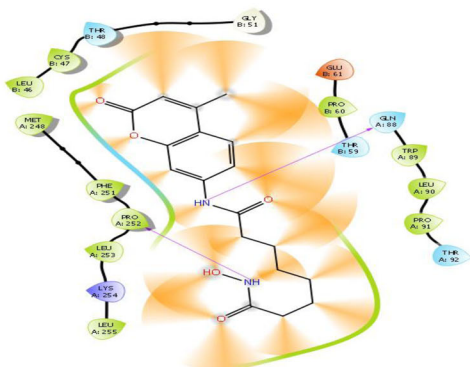
## 102214788 - 6w61 - minimized



## 10781960 - 6w61 - minimized



## 53393956 - 6w61 - minimized



- |  |   |
|--|---|
| <span style="color: red;">●</span> Charged (negative)    | <span style="color: lightblue;">●</span> Polar                |
| <span style="color: orange;">●</span> Charged (positive) | <span style="color: grey;">●</span> Unspecific residue        |
| <span style="color: green;">●</span> Glycine             | <span style="color: blue;">●</span> Water                     |
| <span style="color: yellow;">●</span> Hydrophobic        | <span style="color: red;">●</span> Hydration site             |
| <span style="color: grey;">●</span> Metal                | <span style="color: red;">X</span> Hydration site (displaced) |
| <span style="color: red;">---</span> Distance            | <span style="color: red;">-</span> Pi-cation                  |
| <span style="color: red;">-</span> H-bond                | <span style="color: red;">-</span> Salt bridge                |
| <span style="color: green;">-</span> Halogen bond        | <span style="color: red;">○</span> Solvent exposure           |
| <span style="color: blue;">-</span> Metal coordination   |   |
| <span style="color: green;">-</span> Pi-Pi stacking      |   |

10

Figure 1. The interaction diagram of top five ligands with the NSP10/NSP16 Methyltransferase protein based Dock.

with ligands (mesh surface and solid surface) is present in Supporting Information Figure S2. Amino acid residues Leu, Ala, Val, Thr, Lys and Asp of active site of chain-B Phosphatase forms hydrogen bonding with docked ligands and other amino acid residues shows hydrophobic interaction. The docking scores of Phosphatase are  $-2.38$  and  $-4.86$  of standard drugs Remdisivire and Hydroxychloroquine and  $-8.63$ ,  $-8.22$ ,  $-7.81$ ,  $-7.72$  and  $-7.48$  kcal/mol of coumarin derivatives with ligands PubChem ID: 54730083, 53393956, 3758198, 88279989 and 5359550, respectively (Figure 3 and Table 1), here again coumarin derivatives are showing better result that experimentally proved drugs. Three

dimensional representation of active site of Phosphatase enzyme with all five ligands (mesh surface and solid surface) represented in Supporting Information Figure S3. Binding pocket's amino acid residues Glu, His, Gln and Pro; of Main Protease forms hydrogen bonding with all five ligands. The docking score of ligands PubChem ID: 101223868, 9818076, 43000, 11616886 and 23618487 with Main Protease are  $-7.30$ ,  $-6.33$ ,  $-6.24$ ,  $-6.23$  and  $-6.01$  kcal/mol, respectively (Figure 4 and Table 1), and  $-3.23$  and  $-1.75$  kcal/mol with standard drugs Remdisivire and Hydroxychloroquine respective again showing less docking score than coumarin derivatives. Mesh surface and solid surface 3D

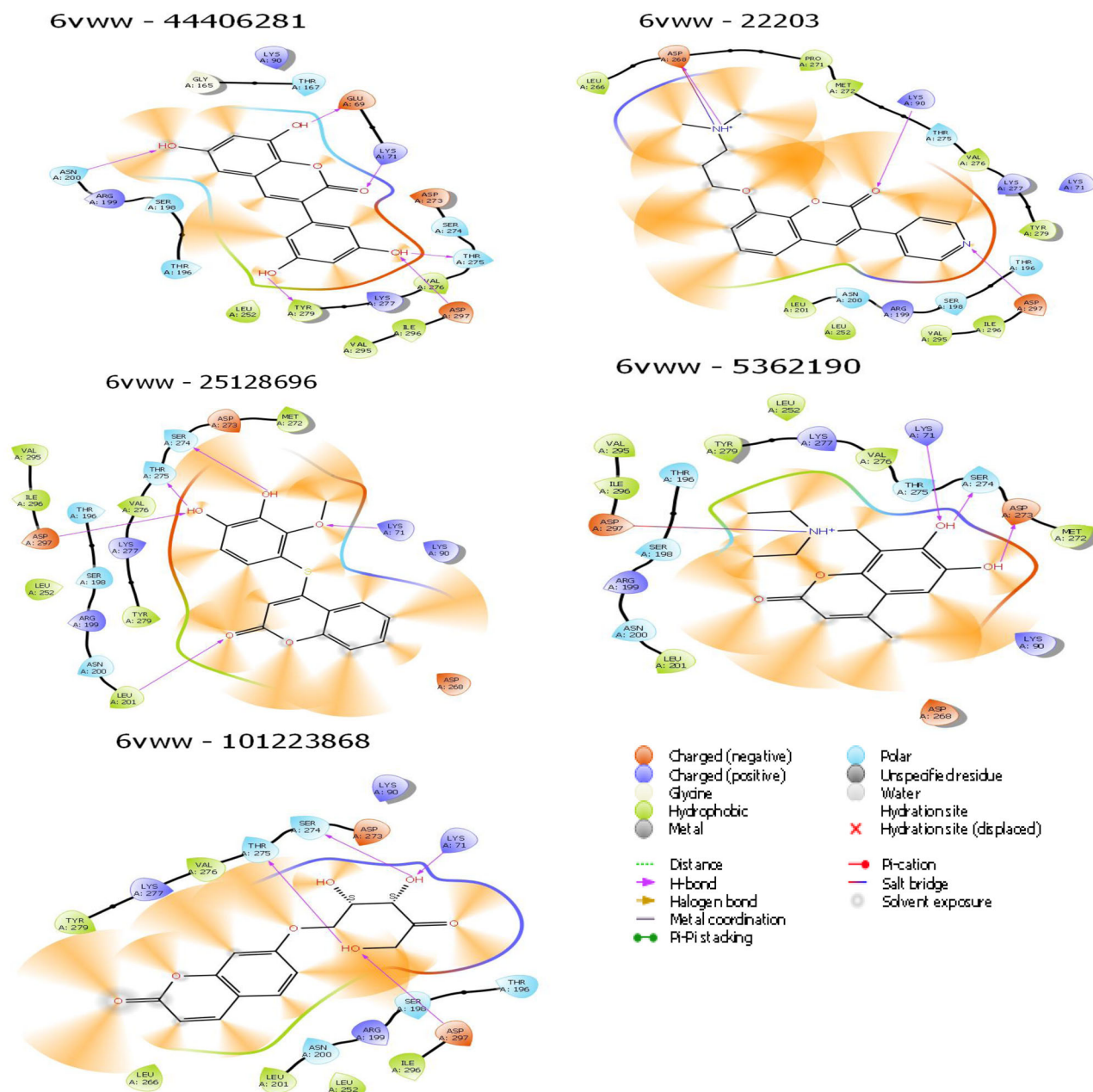


**Figure 2.** The interaction diagram of top five ligands with the Endoribonuclease Protein.

representation of Main Protease and ligands is given in Supporting Information Figure S4. So, Coumarin derivatives are showing better docking score than experimentally proved standard drugs Remdesivir and Hydroxychloroquine for covid-19 treatment.

### 3.2. Estimation of binding free energy

The calculations of MM/GBSA were performed to estimate the relative binding affinity of ligands to the receptor. The top five compounds of NSP10/NSP16 Methyltransferase (MTase), Endoribonuclease (endoU), ADP ribose Phosphatase and Main Protease binding-free energy values are in Table 1. Coumarin derivatives with good docking scores were showed good

binding free energy with their respective receptors. So, these coumarin derivatives may be a potent inhibitor of SARS CoV-2.

### 3.3. ADME/T properties analysis

*In silico* pharmacokinetic and pharmacodynamics properties of the coumarin derivatives calculated by using QikProp utility of Maestro 12.0. The top five docked compounds of each enzyme showed the best ADME/T score (Table 2). It predicts the drug-likeness feature of ligands.

### 3.4. Lipinski rule of five

Pharmacodynamic and pharmacokinetic properties of ligands define drug-likeness of compounds. Lipinski rule defines

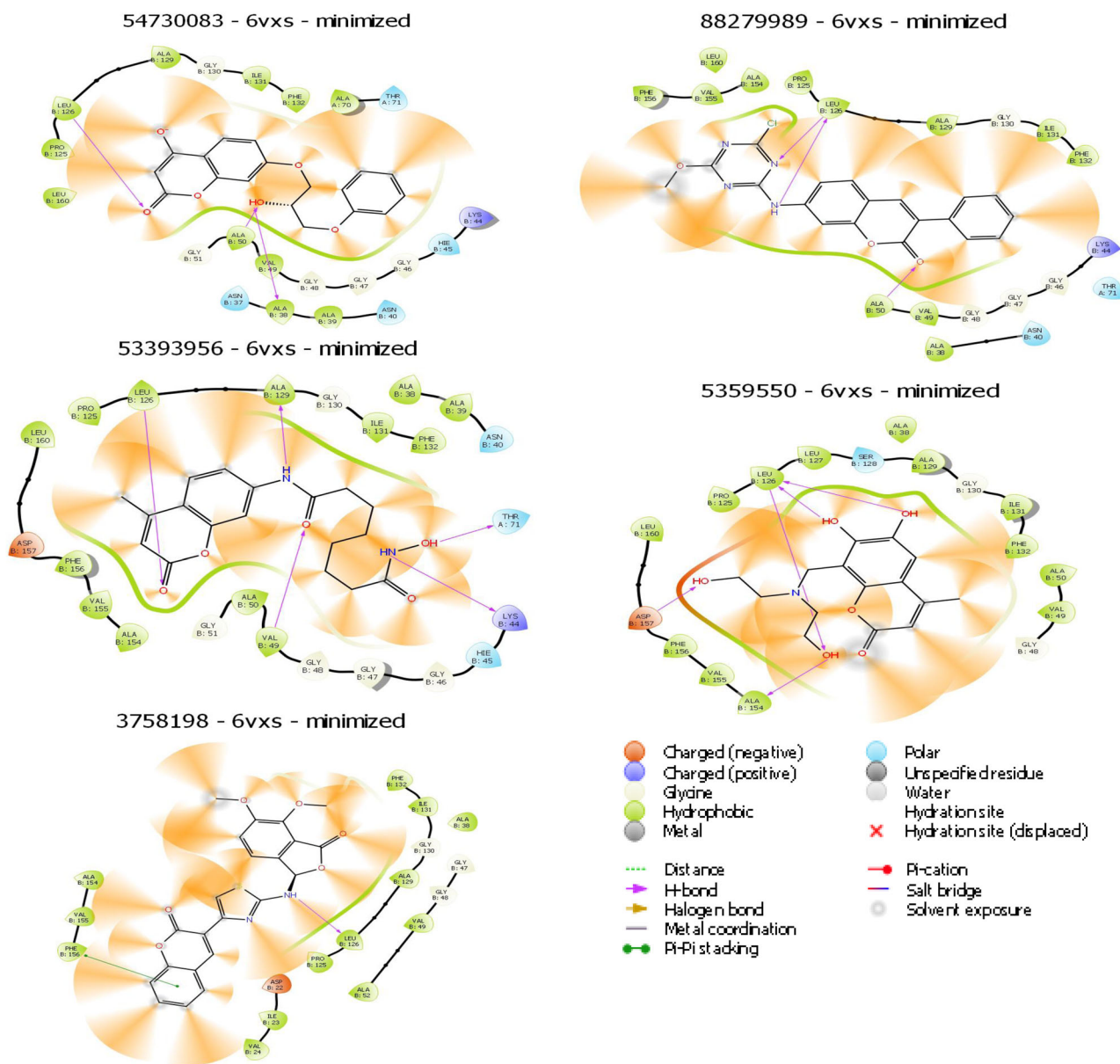


Figure 3. The interaction diagram of top five ligands with the Phosphatase.

numbers for some parameters of compound/s which are molecular weight  $< 500$ ,  $Q\logPo/w < 5$ ,  $donorHB \leq 5$ ,  $accptHB \leq 10$ . The numbers of parameters are in multiples of 5, hence, the rule of five. The compounds which satisfy these numbers for the same parameters are considered as the drug-likeness (Lipinski et al., 1997). ADME/T calculation and rule of five of the top five compounds of each enzyme are given in Table 2.

Interestingly, it was observed that among these top five selected lead molecules of each receptor that was best ranked from the 5% of XP docked molecules, i.e., 20 molecules, 7 molecules have been already tested and bioactive compounds. For example, the second ligand of the Main Protease was 7-[(3-anilino-propylamino)methyl]coumarin (PubChem ID: 9818076) which has a  $-6.33$  docking score,  $-59.83$  MMGBSA binding free energy and 13 ADMET score and has bioassay (PubChem bioassay: 64004) with dopamine

receptor. The third compound of Protease was 7-(3-chlorobenzyl)oxy-4-(methylaminomethyl)coumarin Pubchem ID: 11616886) has bioassay ((PubChem bioassay: 302408) shows the inhibition of human recombinant MAOA expression. The second ligand of Phosphatase is N'-hydroxy-N-(4-methyl-2-oxochromen-7-yl)octanediamide (Pubchem ID: 53393956) has bioassay as anticancer. Third ligand of Phosphatase is 3-[2-[(4,5-dimethoxy-3-oxo-1H-2-benzofuran-1-yl)amino]-1,3-thiazol-4-yl]chromen-2-one (Pubchem ID: 3758198) has bioassay as P53 inhibitor.

Where,

MW = Molecular weight- 130.0–725.0

$\log S$  = Predicted aqueous solubility

$\log o/w$  = Predicted octanol/water partition coefficient-  $-2.0$ – $6.5$

AccptH = Estimated number of hydrogen bonds that would be accepted by the solute from water molecules in an aqueous solution-  $2.0$ – $20.0$



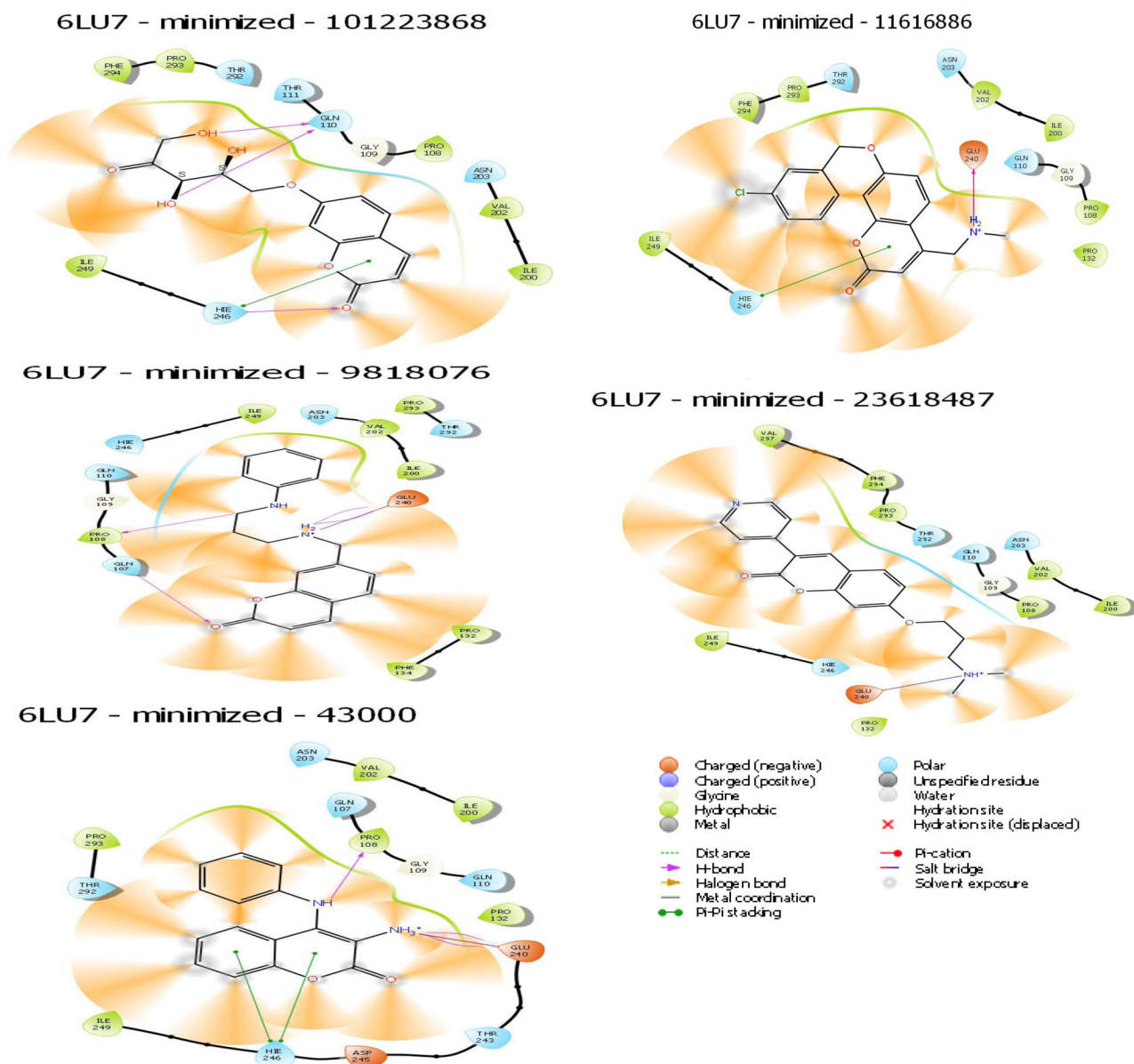


Figure 4. The interaction diagram of top five ligands with the Main Protease.

DonorH = Estimated number of hydrogen bonds that would be donated by the solute to water molecules in an aqueous solution- 0.0–6.0

QPPCaco = Predicted apparent Caco-2 cell permeability in nm/sec. Caco2 cells are a model for the gut-blood barrier- <25 poor, >500 great

QLogBB = Predicted brain/blood partition coefficient- -3.0–1.2

%HumanOralAbs = Predicted human oral absorption on 0 to 100% scale- <25 poor, >80% is high

QLog HERG = Predicted IC50 value for blockage of HERG K+ channels- concern below -5

SASA = Total solvent accessible surface area -300.0–1000.0

FOSA = Hydrophobic component of the SASA- 0.0–750.0

FISA = Hydrophilic component of the SASA (SASA on N, O and H on heteroatoms) 7.0–330.0

PISA =  $\pi$  (carbon and attached hydrogen) component of the SASA- 0.0–450.0

### 3.5. MD simulation analysis

Top first docked ligand of all proteins NSP10/NSP16 Methyltransferase (MTase), Endoribonuclease (endoU), ADP ribose Phosphatase and Main Protease were simulated using the MD package of GROMACS. The analysis of simulated ligand and 7-[(2S,3S)-2,3,5-trihydroxy-4-oxopentoxyl]-1-benzopyran-2-one (PubChem ID: 101223868) steadily proposes the potency against NSP10/NSP16 Methyltransferase (MTase) complex. The graph of RMSD (root mean square deviation) validate that the ligand (PubChem ID: 101223868) and protein MTase gain the complex stability from starting, i.e., within zero ns to 50 ns at 2.29 nm after 50 ns it shows very much fluctuation

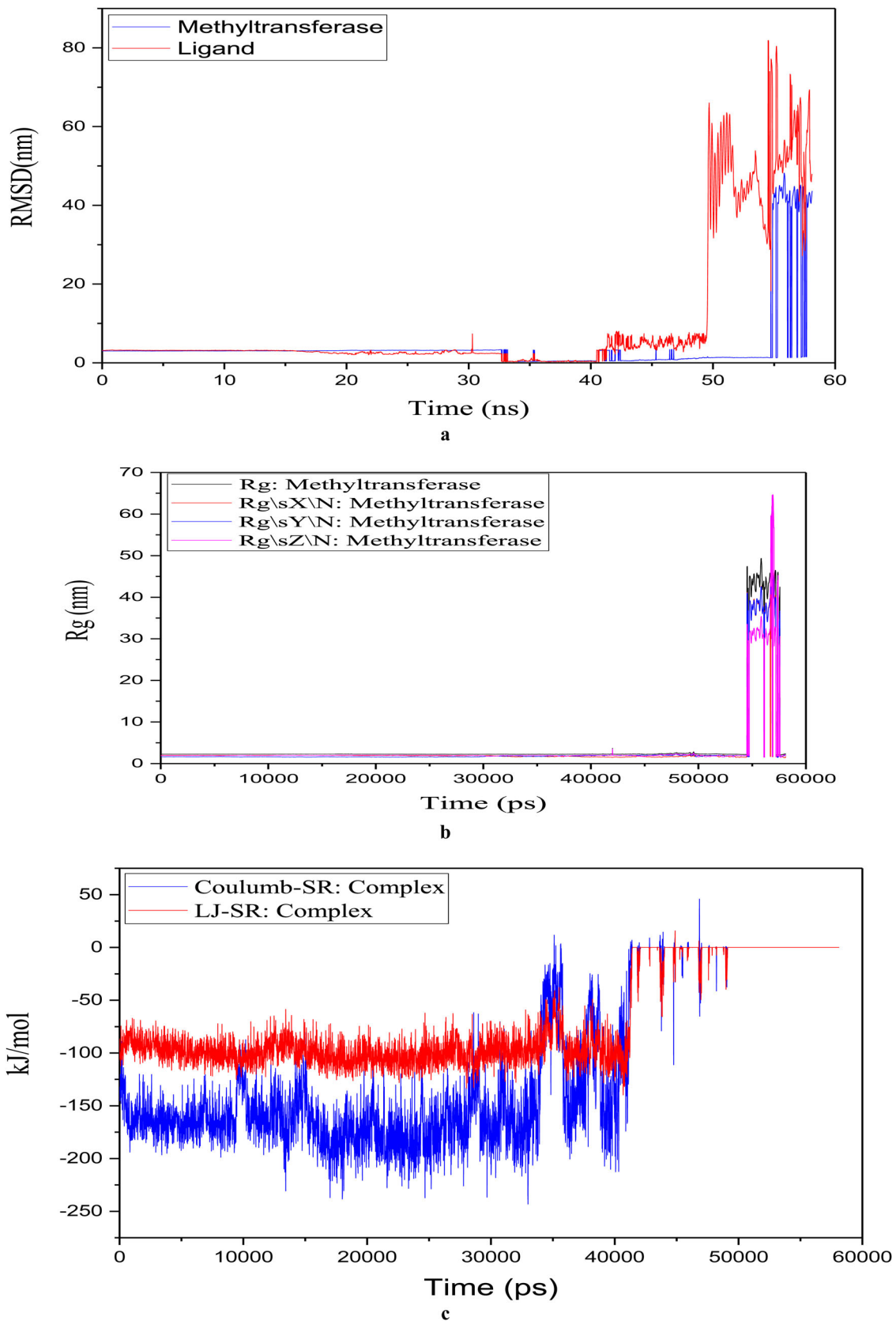


**Figure 5.** Molecular dynamic (MD) simulation graph of NSP10/NSP16 Methyltransferase and ligand (PubChem ID: 101223868) complex (a) RMSD of Methyltransferase and ligand (PubChem ID: 101223868), (b) Radius of Gyration of Methyltransferase and (c) coulomb-SR and LJ-SR energy of complex.

(Figure 5(a)). The radius of Gyration (Rg) (measure compactness of protein) (MTase) showing the steady value of protein from zero ns to 55 ns in Rg, RgX, RgY and RgZ, it means

protein is compactly folded till 55 ns after that protein release their compactness and shows fluctuation (Figure 5(b)) Coulomb-SR energy of MS simulation provide

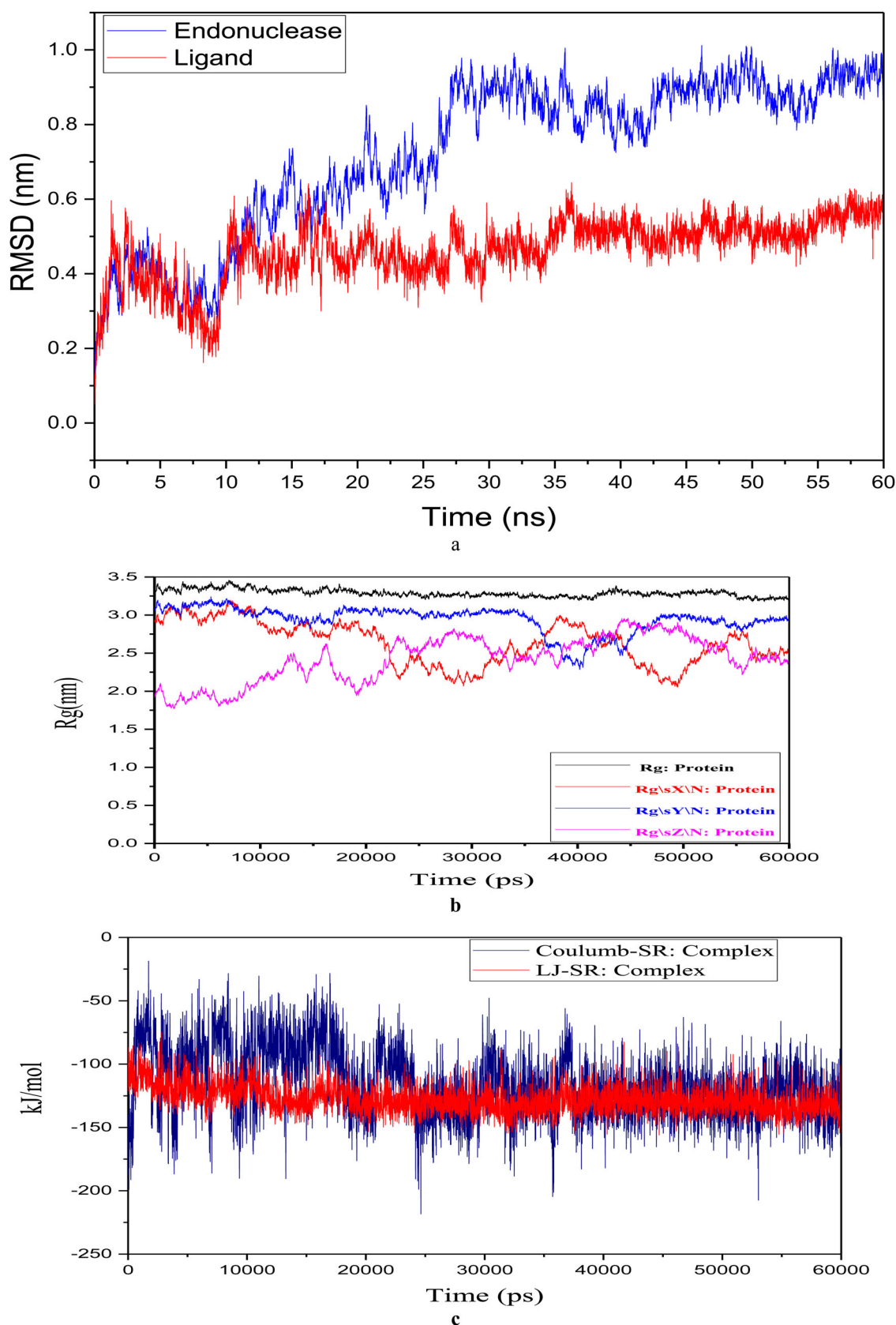


**Figure 6.** MD Simulation graph of (PubChem ID: 44406281) and Endoribonuclease complex, (a) RMSD of (PubChem ID: 44406281) and Endoribonuclease, (b) Radius of Gyration of Endoribonuclease and (c) coulomb-SR and LJ-SR energy of complex.

information about sort rang electrostatic interaction between the atoms. The graph shows the stability of coulomb-SR energy that states that the electrostatic interactions are

constant till 35 ns with atoms of protein–ligand complex, afterward fluctuation occurs in the interaction and the same thing happens in the Lennard–Jones short-range (LJ-SR)

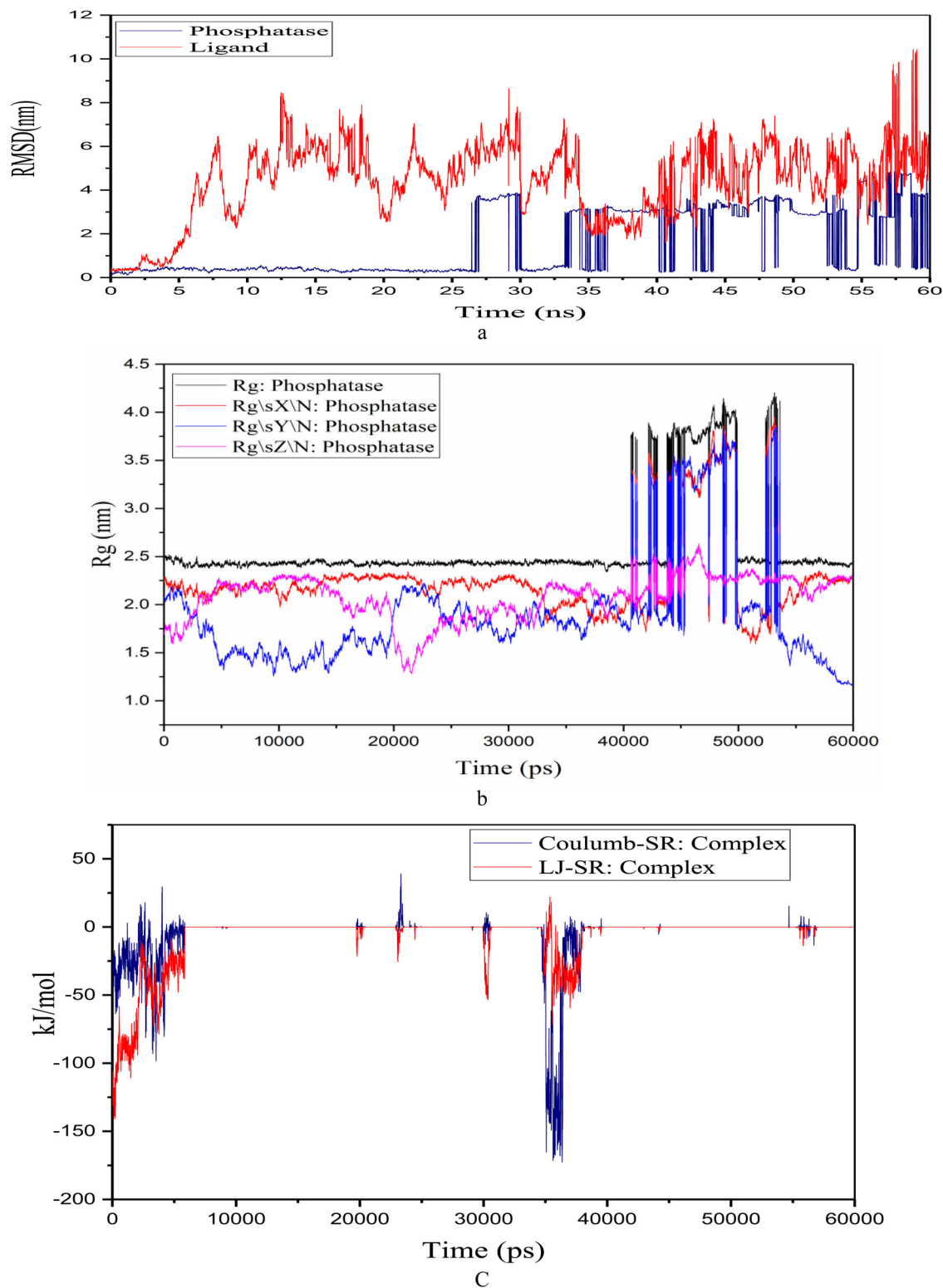


**Figure 7.** MD Simulation graph of ligand (PubChem ID: 54730083) and Phosphatase complex, (a) RMSD of ligand (PubChem ID: 54730083) and Phosphatase, (b) Radius of Gyration of Phosphatase and (c) coulomb-SR and LJ-SR energy of complex.

energy (van der Waals interaction) Figure 5(c). The Coulomb-SR energy and LJ-SR energy shows the binding stability of protein–ligand complex. RMSD, Rg, Coulomb-SR energy and LJ-SR energy of simulation analysis are 2.29 nm, 3.09 nm,  $-135.48$  kJ/mol and  $-106.83$  kJ/mol, respectively, support the potency of ligand against NSP10/NSP16 Methyltransferase. RMSD of both the protein and ligand is showing higher

fluctuations after 50 ns (Figure 5(a)) due to change in the secondary structure and compactness (Figure 5(b)) which lead to increase binding energy higher instability and become separated after 50 ns (Figure 5(c)).

The simulation analysis of docked complex of ligand 3-(3,5-dihydroxyphenyl)-6,8-dihydroxy-1-benzopyran-2-one (PubChem ID: 44406281) and Endoribonuclease shows stability from



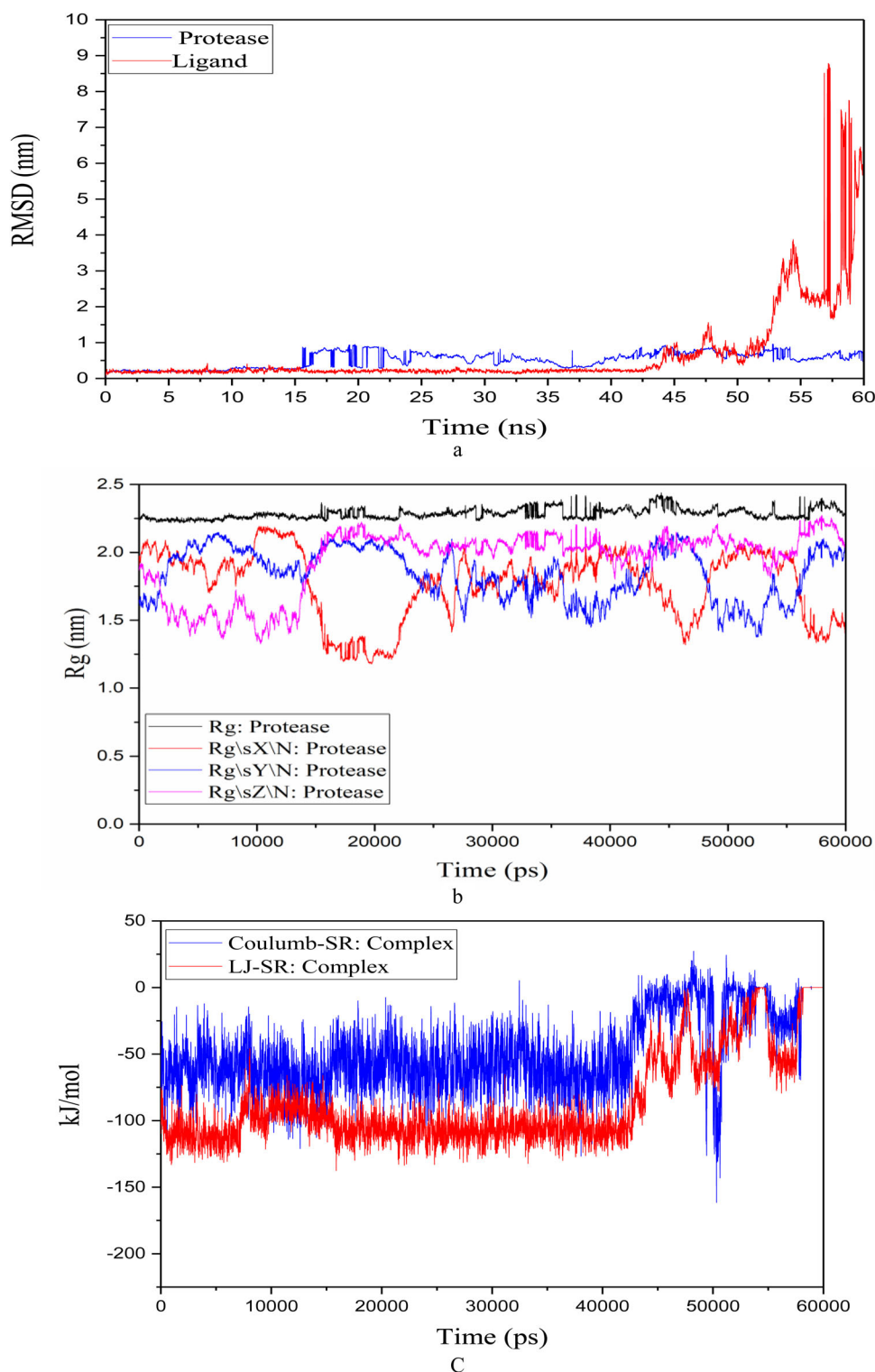


**Figure 8.** MD Simulation graph of ligand (PubChem ID: 101223868) and Main Protease complex, (a) RMSD of ligand ((PubChem ID: 101223868)) and Main Protease, (b) Radius of Gyration of Main Protease and (c) coulomb-SR and LJ-SR energy of complex.

starting (zero ns) to 20 ns afterward the ligand (RMSD-0.1 nm to 0.6 nm) gain more stability than protein (RMSD- 0.1 nm to 1.0 nm) (Figure 6(a)). The Rg of Endoribonuclease shows stability at 3.3 nm though out 60 ns, while the RgX, RgY and RgZ show the fluctuation (Figure 6(b)). The coulomb-SR energy (electrostatic interactions) of Endoribonuclease-ligand complex initially fluctuates afterward it gain binding stability with at about  $-80$  kJ/mol with minor fluctuation (Figure 6(c)). The LJ-SR

energy (van der Waals interaction) showing stability at about  $-120$  kJ/mol. The RMSD, Rg, Coulomb-SR energy and LJ-SR energy of complex are about 0.41 nm, 3.3 nm,  $-80$  kJ/mol and 120 kJ/mol, respectively, reveals the potency of ligand against Endoribonuclease.

Phosphatase and ligand 4-hydroxy-7-(2-hydroxy-3-phenoxypropoxy)chromen-2-one (PubChem ID: 54730083) docked complex was simulated and the result shows stability from

starting at 0.15 nm but ligand shows more fluctuation from 0.15 nm and protein shows RMSD from 0.15 nm to 3.5 nm. Fluctuation in ligand started from 5 ns while in protein 27 ns (Figure 7(a)). Rg of protein is stable at 2.49 nm with small fluctuation; it shows that protein is compactly folded during the ligand binding with a rotation axis of Rg, i.e., RgX, RgY and RgZ show the fluctuation (Figure 7(b)). The coulomb-SR energy and LJ-SR energy of protein-ligand complex initially unstable but after 8 ns it gains stability at  $-20$  kJ/mol, it shows that electrostatic and van der Waal interactions with atoms are stable and shows binding stability (Figure 7(c)). The stable RMSD, Rg, Coulomb-SR energy and LJ-SR energy of complex are 0.15 nm, 2.49 nm,  $-20$  kJ/mol and  $-20$  kJ/mol, respectively, which show the potency of ligand against Phosphatase.

Main Protease (PDB ID: 6LU7) and ligand 7-[(2S,3S)-2,3,5-trihydroxy-4-keto-pentoxycoumarin (PubChem ID: 101223868) simulation reveals the RMSD of ligand and protein binding. It shows that the binding stability of the protein-ligand complex become stable from starting and show the stability up to 53 ns at 0.18 nm. Ligand shows more stability than protein (Figure 8(a)). The Rg of the protein shows stability with small fluctuation it means protein is well folded during the simulation. The rotation RgX, RgY and RgZ axis of protein show high fluctuation it means the protein show the conformational change in the structure (Figure 8(b)). The coulomb-SR and LJ-SR energy of protein-ligand complex show the stability at  $-70$  kJ/mol and  $100$  kJ/mol up to 45 ns afterward became unstable, it means the electrostatic and van der Waal interactions with atoms are stable during the simulation and shows good binding interaction of ligand-protein complex (Figure 8(c)). The stable RMSD, Rg, Coulomb-SR energy and LJ-SR energy of complex are 0.18 nm, 2.49 nm,  $-70$  kJ/mol and  $-100$  kJ/mol, respectively, which show the potency of ligand against Main Protease.

Coumarin derivatives actively interact with taken receptors and showed good docking results for NSP10/NSP16 Methyltransferase (MTase), Endoribonuclease (endoU), ADP ribose Phosphatase and Main Protease and top five compounds of each have docking score from  $-9.00$  to  $-7.97$ ,  $-8.42$  to  $-6.80$ ,  $-8.63$  to  $-7.48$  and  $-7.30$  to  $-6.01$  kcal/mol, respectively. All the enzymes showed good results with different compounds, therefore, less chance to be resistant to other targets. So, the combination therapy of the active compounds may be potent inhibitors of SARS CoV-2. All the simulated ligand-protein complex is showing the binding stability with their respective protein, so, the binding ligands PubChem ID: 101223868, 44406281, 54730083 and 101223868 may be a potent inhibitor of NSP10/NSP16 Methyltransferase (MTase), Endoribonuclease (endoU), ADP ribose Phosphatase and Main Protease of COVID-19, respectively. 7-[(2S,3S)-2,3,5-trihydroxy-4-oxopentoxyl-1-benzopyran-2-one (PubChem ID: 101223868) is the common inhibitor of Main Protease, Endoribonuclease and NSP10/NSP16 Methyltransferase, so the single ligand (PubChem ID: 101223868) is potentially inhibiting three proteins of SARS CoV-2 (Tables 1 and 2). The ligand 7-[(2S,3S)-2,3,5-trihydroxy-4-keto-pentoxycoumarin (PubChem ID: 101223868) may be a more potent inhibitor of COVID-19.

## 4. Conclusion

Methyltransferase (MTase), Endoribonuclease(endoU), ADP ribose Phosphatase and Main Protease enzymes are essential for the viability of SARS CoV-2. Some coumarin derivatives exhibit antiviral activity. Therefore, it has been attempted to identify inhibitors of Methyltransferase (MTase), Endoribonuclease (endoU), ADP ribose Phosphatase and Main Protease enzymes produced by SARS CoV-2 to infect and propagate, by using an *in silico* virtual screening approach. In which, the molecular docking studies were performed for coumarin derivatives. The study yielded five lead compounds of each receptor which have shown promising results against Methyltransferase (MTase), Endoribonuclease(endoU), ADP ribose phosphatase and Main Protease enzymes receptors. Top five compounds of each receptor were used for the estimation of MM/GBSA binding-free energies. All resulted compounds are showing good docking scores and binding free energy with all selected receptors. All ligand molecules which are showing the good result, show admissible properties of the ADME/drug-likeness properties and may be considered as potential drug candidates for prospective research to inhibit SARS CoV-2. The docked top ligand of each receptor was simulated. RMSD, Rg, Coulomb-SR energy and LJ-SR energy of simulation analysis are 2.29 nm, 3.09 nm,  $-135.48$  kJ/mol and  $-106.83$  kJ/mol, respectively, support the potency of ligand (PubChem ID: 101223868) against NSP10/NSP16 Methyltransferase. The RMSD, Rg, Coulomb-SR energy and LJ-SR energy of complex are about 0.41 nm, 3.3 nm,  $-80$  kJ/mol and  $120$  kJ/mol, respectively, reveals the potency of ligand (PubChem ID: 44406281) against Endoribonuclease. The stable RMSD, Rg, Coulomb-SR energy and LJ-SR energy of complex are 0.15 nm, 2.49 nm,  $-20$  kJ/mol and  $-20$  kJ/mol, respectively, which show the potency of ligand (PubChem ID: 54730083) against Phosphatase. And the stable RMSD, Rg, Coulomb-SR energy and LJ-SR energy of complex are 0.18 nm, 2.49 nm,  $-70$  kJ/mol and  $-100$  kJ/mol, respectively, which show the potency of ligand (PubChem ID: 101223868) against Main Protease. All ligand molecules which are showing the good result, show admissible properties of the ADME/T drug-likeness properties and may be considered as potential drug candidates for prospective research to inhibit SARS CoV-2. 7-[(2S,3S)-2,3,5-trihydroxy-4-oxopentoxyl-1-benzopyran-2-one (PubChem ID: 101223868) is the common inhibitor of Main Protease, Endoribonuclease and NSP10/NSP16 Methyltransferase, so, it may be more potent inhibitor of SARS CoV-2.

## Acknowledgement

The authors are grateful to the Indian Institute of Information Technology Allahabad for providing Central computing facility and laboratory support to us.

## Disclosure statement

No potential conflict of interest was reported by the authors.

## Author contributions

Akhilesh Kumar Maurya designed experiments, performed all other experiments and data analysis and prepared the manuscript. Nidhi Mishra guided the study and manuscript preparation.

## Funding

The authors are grateful to the Ministry of Human Resource Development for funding as research fellowship.

## References

- Berendsen, H. J. C., Postma, J. P. M., van Gunsteren, W. F., & Hermans, J. (1981). Interaction models for water in relation to protein hydration. *Intermolecular Forces*, 33, 1–342.
- Berendsen, H. J. C., van der Spoel, D., & van Drunen, R. (1995). GROMACS: A message-passing parallel molecular dynamics implementation. *Computer Physics Communications*, 91(1–3), 43–56. [https://doi.org/10.1016/0010-4655\(95\)00042-E](https://doi.org/10.1016/0010-4655(95)00042-E)
- Bezergiannidou-Balouctsi, C., Litinas, K. E., Malamidou-Xenikaki, E., & Nicolaidis, D. N. (1993). Reactions of 7-(methoxyimino)-4-methyl-2H-chromene-2, 8 (7H)-dione with Phosphorus Ylides. Synthesis of 2-substituted 6-methyl-8H-benzopyrano [7, 8-d] oxazol-8-ones. *Liebigs Annalen Der Chemie*, 1993(11), 1175–1177. <https://doi.org/10.1002/jlac.1993199301190>
- Deng, X., & Baker, S. C. (2018). An “Old” protein with a new story: Coronavirus endoribonuclease is important for evading host antiviral defenses. *Virology*, 517, 157–163. <https://doi.org/10.1016/j.virol.2017.12.024>
- Deng, X., van Geelen, A., Buckley, A. C., O'Brien, A., Pillatzki, A., Lager, K. M., Faaberg, K. S., & Baker, S. C. (2019). Coronavirus endoribonuclease activity in porcine epidemic diarrhea virus suppresses type I and type III interferon responses. *Journal of Virology*, 93(8), e02000. <https://doi.org/10.1128/JVI.02000-18>
- Egan, D., James, P., Cooke, D., & O'Kennedy, R. (1997). Studies on the cytostatic and cytotoxic effects and mode of action of 8-nitro-7-hydroxycoumarin. *Cancer Letters*, 118(2), 201–211. [https://doi.org/10.1016/S0304-3835\(97\)00331-5](https://doi.org/10.1016/S0304-3835(97)00331-5)
- Elmezayen, A. D., Al-Obaidi, A., Şahin, A. T., & Yelekçi, K. (2020). Drug repurposing for coronavirus (COVID-19): in silico screening of known drugs against coronavirus 3CL hydrolase and protease enzymes. *Journal of Biomolecular Structure & Dynamics*, 1–13. <https://doi.org/10.1080/07391102.2020.1758791>
- Hess, B., Kutzner, C., van der Spoel, D., & Lindahl, E. (2008). GROMACS 4: Algorithms for highly efficient, load-balanced, and scalable molecular simulation. *Journal of Chemical Theory and Computation*, 4(3), 435–447. <https://doi.org/10.1021/ct700301q>
- Huang, C., Wang, Y., Li, X., Ren, L., Zhao, J., Hu, Y., Zhang, L., Fan, G., Xu, J., Gu, X., Cheng, Z., Yu, T., Xia, J., Wei, Y., Wu, W., Xie, X., Yin, W., Li, H., Liu, M., ... Cao, B. (2020). Clinical features of patients infected with 2019 novel coronavirus in Wuhan, China. *The Lancet*, 395(10223), 497–506. [https://doi.org/10.1016/S0140-6736\(20\)30183-5](https://doi.org/10.1016/S0140-6736(20)30183-5)
- Hwu, J. R., Singha, R., Hong, S. C., Chang, Y. H., Das, A. R., Vliegen, I., De Clercq, E., & Neyts, J. (2008). Synthesis of new benzimidazole-coumarin conjugates as anti-hepatitis C virus agents. *Antiviral Research*, 77(2), 157–162. <https://doi.org/10.1016/j.antiviral.2007.09.003>
- Jorgensen, W. L., & Duffy, E. M. (2002). Prediction of drug solubility from structure. *Advanced Drug Delivery Reviews*, 54(3), 355–366. [https://doi.org/10.1016/S0169-409X\(02\)00008-X](https://doi.org/10.1016/S0169-409X(02)00008-X)
- Joseph, J. S., Saikatendu, K. S., Subramanian, V., Neuman, B. W., Buchmeier, M. J., Stevens, R. C., & Kuhn, P. (2007). Crystal structure of a monomeric form of severe acute respiratory syndrome coronavirus endonuclease nsp15 suggests a role for hexamerization as an allosteric switch. *Journal of Virology*, 81(12), 6700–6708. <https://doi.org/10.1128/JVI.02817-06>
- Li, J., Abel, R., Zhu, K., Cao, Y., Zhao, S., & Friesner, R. A. (2011). The VSGB 2.0 model: A next generation energy model for high resolution protein structure modeling. *Proteins: Structure, Function, and Bioinformatics*, 79(10), 2794–2812. <https://doi.org/10.1002/prot.23106>
- Ligpprep, M., & Macromodel, G. (2011). *QikProp*. Schrodinger, LLC.
- Lipinski, C. A., Lombardo, F., Dominy, B. W., & Feeney, P. J. (1997). Experimental and computational approaches to estimate solubility and permeability in drug discovery and development settings. *Advanced Drug Delivery Reviews*, 23(1–3), 3–25. [https://doi.org/10.1016/S0169-409X\(96\)00423-1](https://doi.org/10.1016/S0169-409X(96)00423-1)
- Lu, R., Zhao, X., Li, J., Niu, P., Yang, B., Wu, H., Wang, W., Song, H., Huang, B., Zhu, N., Bi, Y., Ma, X., Zhan, F., Wang, L., Hu, T., Zhou, H., Hu, Z., Zhou, W., Zhao, L., ... Tan, W. (2020). Genomic characterisation and epidemiology of 2019 novel coronavirus: Implications for virus origins and receptor binding. *The Lancet*, 395(10224), 565–574. [https://doi.org/10.1016/S0140-6736\(20\)30251-8](https://doi.org/10.1016/S0140-6736(20)30251-8)
- Mark, P., & Nilsson, L. (2001). Structure and dynamics of the TIP3P, SPC, and SPC/E water models at 298K. *The Journal of Physical Chemistry A*, 105(43), 9954–9960. <https://doi.org/10.1021/jp003020w>
- Masters, P. S. (2006). The molecular biology of coronaviruses. *Advances in Virus Research*, 66, 193–292.
- Maurya, S. K., Maurya, A. K., Mishra, N., & Siddique, H. R. (2020). Virtual screening, ADME/T, and binding free energy analysis of anti-viral, anti-protease, and anti-infectious compounds against NSP10/NSP16 methyltransferase and main protease of SARS CoV-2. *Journal of Receptors and Signal Transduction*, 1–8. <https://doi.org/10.1080/10799893.2020.1772298>
- Ministry of Health and Family Welfare India. (2020). <https://www.mohfw.gov.in/>
- Murray, R. D. (2002). The naturally occurring coumarins. In *Fortschritte der chemieorganischernaturstoffe/Progress in the chemistry of organic natural products* (Vol. 83, pp. 1–619). Springer.
- Nicolaidis, D. N., Fylaktakidou, K. C., Litinas, K. E., & Hadjipavlou-Litina, D. (1996). Synthesis and biological evaluation of some 4-(isoxazolonyl or 1, 2, 4-oxadiazolyl) coumarins. *Journal of Heterocyclic Chemistry*, 33(3), 967–971. <https://doi.org/10.1002/jhet.5570330367>
- Olomola, T. O., Klein, R., Mautsa, N., Sayed, Y., & Kaye, P. T. (2013). Synthesis and evaluation of coumarin derivatives as potential dual-action HIV-1 protease and reverse transcriptase inhibitors. *Bioorganic & Medicinal Chemistry*, 21(7), 1964–1971. <https://doi.org/10.1016/j.bmc.2013.01.025>
- Ou, X., Zheng, W., Shan, Y., Mu, Z., Dominguez, S. R., Holmes, K. V., & Qian, Z. (2016). Identification of the fusion peptide-containing region in betacoronavirus spike glycoproteins. *Journal of Virology*, 90(12), 5586–5600. <https://doi.org/10.1128/JVI.00015-16>
- Pavurala, S., Vaarla, K., Kesharwani, R., Naesens, L., Liekens, S., & Vedula, R. R. (2018). Bis coumarinyl bis triazolothiadiazinyl ethane derivatives: Synthesis, antiviral activity evaluation, and molecular docking studies. *Synthetic Communications*, 48(12), 1494–1503. <https://doi.org/10.1080/00397911.2018.1455871>
- Pawar, A. Y. (2020). Combating devastating SARS-COV-2 by drug repurposing. *International Journal of Antimicrobial Agents*, 56(2), 105984. <https://doi.org/10.1016/j.ijantimicag.2020.105984>
- Saikatendu, K. S., Joseph, J. S., Subramanian, V., Clayton, T., Griffith, M., Moy, K., Velasquez, J., Neuman, B. W., Buchmeier, M. J., Stevens, R. C., & Kuhn, P. (2005). Structural basis of severe acute respiratory syndrome coronavirus ADP-ribose-1"-phosphate dephosphorylation by a conserved domain of nsp3. *Structure (London, England: 1993)*, 13(11), 1665–1675. <https://doi.org/10.1016/j.str.2005.07.022>
- Senanavake, S. L. (2020). Drug repurposing strategies for SARS-COV-2. *Future Drug Discovery*, 10, 4155. <https://doi.org/10.4155/fdd-2020-0010>
- Shah, B., Modi, P., & Sagar, S. R. (2020). In silico studies on therapeutic agents for COVID-19: Drug repurposing approach. *Life Sciences*, 252, 117652. <https://doi.org/10.1016/j.lfs.2020.117652>
- Snijder, E. J., Bredenbeek, P. J., Dobbe, J. C., Thiel, V., Ziebuhr, J., Poon, L. L. M., Guan, Y., Rozanov, M., Spaan, W. J. M., & Gorbalenya, A. E. (2003). Unique and conserved features of genome and proteome of SARS-coronavirus, an early split-off from the coronavirus group 2 lineage. *Journal of Molecular Biology*, 331(5), 991–1004. [https://doi.org/10.1016/S0022-2836\(03\)00865-9](https://doi.org/10.1016/S0022-2836(03)00865-9)
- Swiss-Model. (2020). <https://swissmodel.expasy.org/repository/species/2697049>
- Vanommeslaeghe, K., & MacKerell, A. D., Jr. (2012). Automation of the CHARMM General Force Field (CGenFF) I: Bond perception and atom typing. *Journal of Chemical Information and Modeling*, 52(12), 3144–3154. <https://doi.org/10.1021/ci300363c>
- Wang, Z., Chen, X., Lu, Y., Chen, F., & Zhang, W. (2020). Clinical characteristics and therapeutic procedure for four cases with 2019 novel coronavirus pneumonia receiving combined Chinese and Western

- medicine treatment. *Bioscience Trends*, 14(1), 64–68. <https://doi.org/10.5582/bst.2020.01030>
- World Health Organization. (2020a, March 11). WHO Coronavirus disease (COVID-19) outbreak. <https://www.who.int/dg/speeches/detail/who-director-general-s-opening-remarks-at-the-media-briefing-on-covid-19>
- World Health Organization. (2020b, June 8). WHO Coronavirus disease (COVID-19) outbreak. <https://www.who.int/emergencies/diseases/novel-coronavirus-2019>
- Wizard, P. P., Maestro, M., & Phase, I. F. (2009). *Jaguar, and Glide*. Schrödinger, LLC.